Neurobiology of Aging 35 (2014) 2681–2690

Contents lists available at ScienceDirect

Neurobiology of Aging

journal homepage: www.elsevier.com/locate/neuaging

Frontobasal gray matter loss is associated with the *TREM2* p.R47H variant

Elkin O. Luis [a,1], Sara Ortega-Cubero [b,c,1], Isabel Lamet [c], Cristina Razquin [b], Carlos Cruchaga [d], Bruno A. Benitez [d], Elena Lorenzo [b], Jaione Irigoyen [b,c], Alzheimer's Disease Neuroimaging Initiative (ADNI)[2]; Maria A. Pastor [a,c,e], Pau Pastor [b,c,e,*]

[a] *Neuroimaging Laboratory, Division of Neurosciences, Center for Applied Medical Research (CIMA), University of Navarra, Pamplona, Spain*
[b] *Neurogenetics Laboratory, Division of Neurosciences, Center for Applied Medical Research, University of Navarra, Pamplona, Spain*
[c] *Department of Neurology, Clínica Universidad de Navarra, University of Navarra School of Medicine, Pamplona, Spain*
[d] *Hope Center for Neurological Disorders, Department of Psychiatry, Washington University School of Medicine, St Louis, MO, USA*
[e] *Centro de Investigación Biomédica en Red de Enfermedades Neurodegenerativas (CIBERNED), Instituto de Salud Carlos III, Madrid, Spain*

ARTICLE INFO

Article history:
Received 9 January 2014
Received in revised form 6 June 2014
Accepted 10 June 2014
Available online 17 June 2014

Keywords:
Alzheimer
TREM2
Neuroimaging
MRI
Voxel-based morphometry
Genetics
Variant
Mutation

ABSTRACT

A rare heterozygous *TREM2* variant p.R47H (rs75932628) has been associated with an increased risk for Alzheimer's disease (AD). We aimed to investigate the clinical presentation, neuropsychological profile, and regional pattern of gray matter and white matter loss associated with the *TREM2* variant p.R47H, and to establish which regions best differentiate p.R47H carriers from noncarriers in 2 sample sets (Spanish and Alzheimer's Disease Neuroimaging Initiative, ADNI1). This was a cross-sectional study including a total number of 16 *TREM2* p.R47H carriers diagnosed with AD or mild cognitive impairment, 75 AD p.R47H noncarriers and 75 cognitively intact *TREM2* p.R47H noncarriers. Spanish AD *TREM2* p.R47H carriers showed apraxia (9 of 9) and psychiatric symptoms such as personality changes, anxiety, paranoia, or fears more frequently than in AD noncarriers (corrected $p = 0.039$). For gray matter and white matter volumetric brain magnetic resonance imaging voxelwise analyses, we used statistical parametric mapping (SPM8) based on the General Linear Model. We used 3 different design matrices with a full factorial design. Voxel-based morphometry analyses were performed separately in the 2 sample sets. The absence of interset statistical differences allowed us to perform joint and conjunction analyses. Independent voxel-based morphometry analysis of the Spanish set as well as conjunction and joint analyses revealed substantial gray matter loss in orbitofrontal cortex and anterior cingulate cortex with relative preservation of parietal lobes in AD and/or mild cognitive impairment *TREM2* p.R47H carriers, suggesting that *TREM2* p.R47H variant is associated with certain clinical and neuroimaging AD features in addition to the increased *TREM2* p.R47H atrophy in temporal lobes as described previously. The high frequency of pathologic behavioral symptoms, combined with a preferential frontobasal gray matter cortical loss, suggests that frontobasal and temporal regions could be more susceptible to the deleterious biological effects of the *TREM2* variant p.R47H.

1. Introduction

Triggering receptor expressed on myeloid cells 2 (*TREM2*; OMIM: *605086) is a transmembrane glycoprotein which forms a receptor signaling complex with the TYRO protein tyrosine kinase binding protein. *TREM2* is mainly expressed in the microglia of the white matter, hippocampus, neocortex, cerebellum, basal ganglia, corpus callosum, medulla oblongata, and spinal cord (Guerreiro et al., 2013a, 2013b; Paloneva et al., 2002). *TREM2* promotes the production of constitutive inflammatory cytokines in microglia (Bouchon et al., 2000; Lanier and Bakker, 2000), leading to the phagocytosis of cell debris and amyloid (Paloneva et al., 2002;

* Corresponding author at: Neurogenetics Laboratory, Division of Neurosciences, Center for Applied Medical Research (CIMA), University of Navarra School of Medicine, Pío XII 55, 31008-Pamplona, Spain. Tel.: +34 948194700; fax: +34 948194715.
E-mail address: pastorpau@gmail.com (P. Pastor).

[1] These authors contributed equally to this article.

[2] Some of the data used in the preparation of this article were obtained from the Alzheimer's Disease Neuroimaging Initiative (ADNI) database (adni.loni.usc.edu). The investigators within the ADNI contributed to the design and implementation of ADNI and/or provided data but did not participate in the analysis or writing of this report. A complete listing of ADNI investigators can be found at: http://adni.loni.usc.edu.

0197-4580/$ – see front matter © 2014 Elsevier Inc. All rights reserved.
http://dx.doi.org/10.1016/j.neurobiolaging.2014.06.007

Takahashi et al., 2005). Recessive *TREM2* loss-of-function mutations cause Nasu-Hakola disease (NHD) or polycystic lipomembranous osteodysplasia with sclerosing leukoencephalopathy (MIM 221770), which is characterized by early-onset frontal-like dementia and bone involvement (Hakola, 1972; Montalbetti et al., 2005; Paloneva et al., 2002). In addition, some families with inherited recessive frontotemporal-like dementia (FTD-like) with leukodystrophy without bone involvement carry *TREM2* mutations (Guerreiro et al., 2013a, 2013b; Montalbetti et al., 2005).

Recently, a rare *TREM2* variant (p.R47H; rs75932628-T) has been associated with susceptibility to late-onset Alzheimer's disease (AD) with an effect size similar to that of *APOE* ε4 (Guerreiro et al., 2013a, 2013b; Jonsson et al., 2013; Ruiz et al., 2014). Although the role of p.R47H in protein function is not yet known, it has been proposed that this amino acid change at the immunoglobulin-like domain could impair the anti-inflammatory function of *TREM2* and facilitate amyloidogenic inflammatory response supported by its co-localization with amyloid plaques (Melchior et al., 2010). Pathologic examination of brains with *TREM2* rare variants including p.R47H revealed that all were in advanced AD (Braak stage 6) and most had typical findings with no distinguishing features except for the presence of mild Lewy body and TAR DNA-binding protein 43 disease in 2 of them (Guerreiro et al., 2013a, 2013b). Interestingly, *TREM2* rare variants have also been inconsistently associated with other neurodegenerative diseases such as FTD, Parkinson's disease or amyotrophic lateral sclerosis (Rayaprolu et al., 2013; Ruiz et al., 2014; Cady et al., 2014; Thelen et al., 2014). These results suggest that *TREM2* dysfunction in AD brains can lead to more deleterious effects in certain brain regions such as frontal lobes or basal ganglia than in subjects with AD not carrying *TREM2* damaging variants. However, no *TREM2* p.R47H-associated phenotypical clinical and neuropsychological features have been systematically described to date, in part because of the low frequency of the *TREM2* mutations (Reitz and Mayeux, 2013). In addition, *TREM2* expression studies across the human brain have demonstrated significant regional differences (Forabosco et al., 2013), suggesting that certain cortical and subcortical brain regions could have an increased susceptibility owing to the mutant *TREM2* protein. In fact, a tensor-based morphometry study of the temporal lobe has recently reported 1.4%–3.3% annual rates of increase of brain volume loss in this area in *TREM2* p.R47H AD carriers compared with noncarriers (Rajagopalan et al., 2013). However, no whole brain voxel-based morphometry (VBM) studies on *TREM2* variant carriers including gray and white matter are available.

Therefore, we aimed to investigate whether differences in clinical presentation and neuropsychological profile were associated with the *TREM2* variant p.R47H, and to determine the regional pattern of gray matter and white matter loss associated with the *TREM2* p.R47H variant, to elucidate which regions best differentiate *TREM2* p.R47H carriers from AD and/or MCI noncarriers and from cognitively intact noncarriers p.R47H in 2 populations (Spanish and Alzheimer's Disease Neuroimaging Initiative, ADNI1). For that, we performed brain magnetic resonance imaging (MRI) VBM analysis separately in 2 sample sets (the Spanish set and the ADNI1 set, to replicate the findings). After performing a full factorial 2-way ANOVA that showed no specific intra-sample set morphometric differences, conjunction and joint analyses of both sets were also performed.

2. Methods

2.1. Subjects

2.1.1. Genotyping of TREM2 p.R47H variant and subject selection

2.1.1.1. Spanish set. Subjects with probable AD (n = 550) and healthy controls (n = 550) recruited at the Memory Disorders Unit, Department of Neurology, Clínica Universidad de Navarra, School of Medicine (Pamplona, Spain) were screened for *TREM2* p.R47H with a specifically designed KASPar assay as described (Benitez et al., 2013). Early-onset AD subjects with relevant genetic AD variants were excluded by pooled-DNA next generation sequencing of exonic and flanking sequences in *APP*, *PSEN1*, *PSEN2*, *MAPT*, and *GRN* genes (Jin et al., 2012). Before their participation, written informed consent was obtained from participant subjects or relatives.

2.1.1.2. ADNI1 set. The *TREM2* p.R47H variant was initially determined by direct genotyping (KASPar) in all the ADNI1 DNA as described (Benitez et al., 2013). As whole-genome sequencing data had recently been released for the ADNI1 samples, we used these data to validate and confirm the presence of *TREM2* variant. ADNI1 GWAS data (common variants Illumina 610) as well as HapMap data were used to calculate the principal component factors from population stratification using EIGENSOFT version 5.0.1 (Patterson et al., 2006) to assure that all ADNI1 subjects had a European descent.

2.1.1.3. AD and MCI definition. All AD subjects (p.R47H carriers and noncarriers from both sets) fulfilled the NINCDS-ADRDA research criteria for probable AD (McKhann et al., 1984). All AD patients from ADNI were in mild AD stages (Mini Mental State Examination [MMSE] scores between 20–26 and Clinical Dementia Rating [CDR] of 0.5–1). ADNI MCI subjects were defined as patients having memory complaints, low scores adjusted for education of Wechsler Memory Scale Logical Memory II b, MMSE scores between 24 and 30, CDR = 0.5, absence of significant impairment in other cognitive domains, absence of dementia, and essentially preserved activities of daily living (adni.loni.usc.edu). MCI subjects from ADNI data set were followed prospectively at 0, 6, 12, 18, 24, and 36 months allowing to track the conversion from MCI to AD (Supplementary Table 6). When available, decreased levels of ß-amyloid peptide 1-42 ($A\beta_{1-42}$) in cerebrospinal fluid (≤192 pg/mL) were also considered as an AD predictor (Supplementary Table 6; Shaw et al., 2009).

2.1.2. Subjects selected for the study

2.1.2.1. Spanish set. We found 9 AD heterozygous carriers of the *TREM2* p.R47H, expanding our previously reported series (series details reflected in the Supplementary material) (Benitez et al., 2013). To investigate whether *TREM2* p.R47H was associated with specific clinical and neuroimaging characteristics, 9 AD *TREM2* p.R47H carriers (median age = 69.3 years, range = 57–84 years, 55.5% male) were compared with 48 AD p.R47H noncarriers (median age = 70 years, range = 52–83 years, 52% male) and 48 cognitively intact p.R47H noncarriers (median age = 69.5 years, range = 55–82 years, 48% male). These groups have similar gender proportion, age at onset, disease duration, and age at evaluation to those of AD p.R47H carriers.

2.1.2.2. ADNI1 set. Neuroimaging and clinical data were obtained from ADNI1 database (adni.loni.usc.edu) subjects screened for the presence of *TREM2* p.R47H (Supplementary material). Nine *TREM2* p.R47H carriers (median age = 81 years, range = 71–91 years, 55.5% male) were compared with 27 cognitively impaired *TREM2* p.R47H noncarriers (median age = 78 years, range = 70–91 years, 55.5% male) and 27 cognitively intact p.R47H noncarriers (median age = 79 years, range = 70–90, 55.5% male; Table 1). Seven *TREM2* p.R47H carriers and 20 *TREM2* p.R47H noncarriers belonged to the MCI research group (Supplementary Table 6). Among these MCI subjects, 13 (4 carriers and 9 noncarriers) converted clinically to AD during follow-up, 2 MCI *TREM2* p.R47H noncarriers showed an MMSE decrease ≥5 points, 5 (1 carrier and 4 noncarriers) showed a cerebrospinal fluid biomarker signature suggestive of AD ($A\beta_{1-42} \leq$

Table 1
Comparison of demographic and clinical data between *TREM2* p.R47H carriers and noncarriers from both sets

	AD/MCI *TREM2* p.R47H carriers	AD/MCI *TREM2* p.R47H noncarriers	Healthy p.R47H *TREM2* noncarriers	Corrected *p*-values
n				
MCI	7	20		
AD	11	55		
Total	18	75	75	
Gender (% female)				
MCI	28.6	23.5		
AD	54.5	60.3		
Total	44.4	52	49.3	NS
Age at evaluation, y				
MCI	78.5 ± 7.1 (70.4–90.9)	78.7 ± 5.1 (72.6–90.6)		
AD	71.7 ± 10.6 (57.5–84)	71.0 ±7.9 (52.1–90.9)		
Total	74.3 ± 9.8 (57.5–90.9)	72.8 ± 8 (52.1–90.9)	70.6 ± 8.8 (55–89.8)	NS
Age at onset, y				
MCI	77.2 ± 6.5 (69.9–89.1)	74.9 ± 4.5 (72.1–89.4)		
AD	67.9 ± 9.9 (55.6–80)	68.2 ± 8.1 (48.5–89.2)		
Total	71.6 ± 9.7 (55.6–89.1)	70.3 ± 8.3 (48.5–89.4)	—	NS
Positive family history (%)[a]				
MCI	71.4	47.1		
AD	50	53.1		
Total	58.8	51.5	48	NS
MMSE				
MCI	22.9 ± 6.4 (11–29)	26.5 ± 3.9 (15–30)		
AD	14.6 ± 8.2 (4–26)	19.6 ± 4.8 (8–29)		
Total	18 ± 8.4 (4–29)	21.16 ± 5.43 (8–30)	—	0.013[c]
Scheltens scale				
MCI	6.4 ± 3.8 (0–13)	11.3 ± 5.9 (0–24)		
AD	8.7 ± 5.2 (5–21)	8.4 ± 6.4 (0–27)		
Total	7.69 ± 4.64 (0–21)	9 ± 6.37 (0–27)	—	NS
APOE (%) (n MCI/n AD)				
23	0	1.33 (0/1)	65.27	<0.001[b]
24	0	1.33 (0/1)	1.38	
33	50 (2/7)	40 (10/20)	26.38	
34	38.88 (3/4)	42.66 (8/24)	5.55	
44	11.12 (2/0)	14.68 (2/9)	2.77	

Numerical data are presented as mean ± standard deviation (range). Categorical data are presented as percentage.
Key: AD, Alzheimer's disease; MCI, mild cognitive impairment; MMSE, Mini Mental State Examination; NS nonsignificant statistical differences.
[a] First-degree family history of dementia.
[b] Distribution of APOE genotype frequencies was statistically different between cognitively impaired (both AD/MCI p.R47H carriers and noncarriers) and healthy subjects for all genotypes except for APOE 24 for which showed no statistically significant differences in frequency distribution.
[c] Other neuropsychological tests did not show any significant difference between both AD and/or MCI groups. The level of significance considered was 0.05. All *p*-values were two sided. Bonferroni correction was applied for multiple comparisons.

192 pg/mL) and the other 7 (2 carriers and 5 noncarriers) remained cognitively stable during follow-up (Shaw et al., 2009).

TREM2 p.R47H noncarriers with MCI, AD, and cognitively intact subjects were selected with same gender proportion, age at onset, disease duration, and age at evaluation to those of AD/MCI p.R47H carriers. All ADNI1 subjects selected for our study had European ancestry. The Review Board at the University of Navarra (Pamplona, Spain) and ADNI1 approved the study.

Thus, considering both sets the total study sample was composed as follows: 18 AD/MCI p.R47H carriers, 75 AD/MCI p.R47H noncarriers, and 75 cognitively intact p.R47H noncarriers (Table 1).

2.1.3. Clinical data and neuropsychological assessment

2.1.3.1. Spanish set. All AD subjects (p.R47H carriers and noncarriers) underwent a standard medical interview and a neurologic examination by a neurologist specializing in cognitive disorders (Maria A. Pastor, Sara Ortega-Cubero, and Pau Pastor). Clinically relevant data, such as first-degree history of dementia or other neurologic disorders were recorded from their family relatives (Table 1). MRI scans were performed at the visit when diagnosis of MCI or AD was made. When the degree of cognitive decline was not severe (which was the situation with 62% of the sample), a complete neuropsychological examination was performed by a trained neuropsychologist (Isabel Lamet). The neuropsychological battery included the following tests: MMSE (Folstein et al., 1975), long version of the Geriatric Depression Rating Scale (Yesavage et al., 1982), semantic verbal fluency (list of animals) (Parkin and Java, 1999), Trail Making Test parts A and B (Tombaugh, 2004), Alzheimer's disease assessment scale Word List (Mohs et al., 1997), and 60-item Boston Naming Test (Williams et al., 1989).

2.1.3.2. ADNI1's set. Thirty-six MCI and/or AD ADNI1 subjects (p.R47H carriers and noncarriers) also underwent a cognitive assessment. Since the neuropsychological battery was not complete in all the subjects we selected the tests with more data available. Thus, the tests selected were the following (the number of subjects who underwent this test is reflected in brackets): the CDR sum of boxes (CDR-SOB) scale as a measure of cognitive and functional impairment (Morris, 1993; n = 36), the MMSE (Folstein et al., 1975), the Alzheimer's disease assessment scale Word list (Mohs et al., 1997; n = 36), Geriatric Depression Rating Scale short form (Yesavage et al., 1982; n = 36), semantic verbal fluency (list of animals) (Parkin and Java, 1999; n = 27), Trail Making Test-A and B (Tombaugh, 2004; n = 27), and the 30-item Boston Naming Test (Williams et al., 1989; n = 27).

Two composite scores for memory and executive function (ADNI-MEM and ADNI-EF) were also recorded (Crane et al., 2012; Gibbons et al., 2012; n = 34 and 33; respectively). More details

Table 2
Comparison of clinical data between Spanish AD *TREM2* p.R47H carriers and noncarriers

	AD p.R47H *TREM2* carriers	AD p.R47H *TREM2* noncarriers	Corrected *p*-values
n	9	48	
First symptom			
Forgetfulness	(7/9) 77.8	(44/48) 91.7	NS
Depression	(2/9) 22.2	(0/48) 0	NS
Others[a]	(0/9) 0	(4/48)	NS
Early signs/symptoms[b]			
Psychiatric symptoms	(9/9) 100	(22/48) 45.8	0.039
Personality changes	(8/9) 88.9	(18/48) 37.5	NS
Spatial disorientation	(8/9) 88.9	(16/48) 33.3	0.01
Memory impairment	(9/9) 100	(47/48) 97.9	NS
Aphasia	(9/9) 100	(37/48) 77.1	NS
Apraxia	(9/9) 100	(15/48) 48	<0.0001
Agnosia	(3/9) 33.3	(12/48) 25	NS
Dysexecutive syndrome	(7/9) 71.4	(38/48) 79.2	NS
Primitive reflexes	(6/9) 57.1	(23/48) 41.7	NS
Parkinsonian signs	(6/9) 66.7	(7/48) 14.6	0.039

Data are presented as frequency and percentage and compared using the exact $\chi 2$-test.
Key: NS, nonsignificant statistical differences.
[a] This category included the following symptoms: nervousness, aphasia, and spatial disorientation.
[b] Early signs and/or symptoms were considered when they appeared during the first 2 years after disease onset.

about the neuropsychological assessment can be found on the ADNI website www.adni.loni.usc.edu.

2.2. Demographic, clinical, and neuropsychological data analysis

The normality of the distribution and variance homogeneity of the numerical variables included in the study was tested using the Shapiro-Wilk and Levene tests, respectively. ANOVA was applied to analyze differences between the means of these variables among the 3 study groups (AD/MCI *TREM2* p.R47H carriers, AD/MCI *TREM2* p.R47H noncarriers, and healthy p.R47H *TREM2* noncarriers). A *t* test was applied to search for differences between means when only the 2 AD/MCI study groups (AD/MCI *TREM2* p.R47H carriers and AD/MCI *TREM2* p.R47H noncarriers) were considered. Pure discrete counting variables were compared using the exact $\chi 2$-test.

All *p*-values were 2-sided and all analyses were carried out using SPSS 15.0 software for Windows (SPSS Inc, Chicago, Illinois, USA) (Tables 1–3).

Subsequently, neuropsychological data from both sets (Spanish and ADNI1) were analyzed to increase the statistical power. Both AD/MCI p.R47H carriers and AD/MCI p.R47H noncarriers subgroups were matched as following: each AD/MCI p.R47H carrier with 3 AD/MCI p.R47H noncarriers with similar gender, age at evaluation, and age at onset to avoid a confounding effect of different distribution of neuropsychological variables between groups. After that, a conditional logistic regression model analyzing the relationship between neuropsychological variables and TREM2 p.R47H status was individually applied for each neuropsychological test. The analysis was carried out using the program Epi InfoTM 7.1.2.0. Bonferroni correction was applied for multiple comparisons in all cases. The level of significance considered was $p < 0.05$ (Table 3).

2.3. Neuroimaging assessment

2.3.1. Data acquisition

2.3.1.1. Spanish set. Two of the 18 p.R47H carriers did not tolerate the 1.5T MRI scan because of claustrophobia. Sixteen of 18 p.R47H carriers (ADNI1 = 9, Spanish = 7), 74 cognitive impaired p.R47H noncarriers (ADNI1 = 27, Spanish = 47), and 74 cognitively intact p.R47H noncarriers (ADNI1 = 27; Spanish = 47) underwent MRI scans. MRI studies of the Spanish subjects were all obtained on a 1.5T Siemens Symphony scanner (Siemens, Erlaghen, Germany). High-resolution volumetric images were acquired in a T1-weighted MR sequence in-plane resolution voxel size $1 \times 1 \times 1$.

2.3.1.2. ADNI1 set. The T1-weighted images from ADNI were obtained using 3 different 1.5T scanners. Nine AD *TREM2* carriers, 12 AD *TREM2* noncarriers, and 18 cognitively intact p.R47H noncarriers' images were acquired in a 1.5T Siemens Symphony scanner. Ten of the remaining AD *TREM2* noncarriers and the healthy control images were acquired in a 1.5T General Electric Medical Systems equipment. Finally, 5 AD/MCI *TREM2* noncarriers and 4 healthy control images were obtained with a Philips Medical Systems. Because the 3 image collections had different voxel sizes (X_1 = 1.2 mm, Y_1 = 1.2 mm, Z_1 = 1.2 mm; X_2 = 0.92 mm; Y_2 = 0.92 mm,

Table 3
Conditional logistic regression model analyzing the relationship between neuropsychological variables and *TREM2* p.R47H status

Cognitive domain	Neuropsychological test	Coefficient	Standard error	Z statistic	Uncorrected *p*-value	Odds ratio	95% CI
Daily living activities	CDR[a]	1.3780	1.1837	1.1641	0.2444	3.9669	0.3898–40.3685
	MMSE[b]	−0.1593	0.0620	−2.5706	0.0102[c]	0.8257	0.7552–0.9629
Psychiatric symptoms	GDS 15[a]	0.1125	0.1880	0.5980	0.5498	1.1190	0.7741–1.6177
	GDS 30[d]	0.0578	0.1077	0.5370	0.5913	1.0596	0.8579–1.3086
Executive functions	ADNI_EF[a]	−0.0614	0.4157	−0.1477	0.8826	0.9405	0.4164–2.1240
	Semantic verbal fluency[b]	0.0000	0.1250	0.0000	1.0000	1.0000	0.7827–1.2776
	Trail making A[b]	−0.0107	0.0075	−1.4304	0.1526	0.9893	0.9749–1.0040
	Trail making B[b]	−0.0055	0.0051	−1.0899	0.2758	0.9945	0.9846–1.0044
Memory	ADAS word list						
	Third trial[b]	0.0025	0.1718	0.0143	0.9886	1.0025	0.7159–1.4037
	Differed[b]	−0.0245	0.1725	−0.1420	0.8871	0.9758	0.6958–1.3684
	ADNI_MEM[d]	−0.2230	0.4926	−0.4528	0.6507	0.8001	0.3046–2.1012
Language	Boston (30 items)[a]	0.1001	0.1272	0.7872	0.4312	1.1053	0.8614–1.4182
	Boston (60 items)[d]	−0.1280	0.1145	−1.1182	0.2635	0.8799	0.7030–1.1011

Key: ADAS, Alzheimer's disease assessment scale; ADNI1, Alzheimer's Disease Neuroimaging Initiative; CDR, Clinical Dementia Rating; CI, confidence interval; GDS, Geriatric Depression Rating Scale; MMSE, Mini Mental State Examination.
[a] ADNI1 set.
[b] ADNI1 and Spanish set.
[c] *p*-value = 0.1326 after correcting for multiple comparisons.
[d] Spanish set.

Z_2=0.92 mm; and $X_3 = 0.93$ mm; $Y_3 = 0.93$ mm; $Z_3 = 0.93$ mm), all T1-weighted images were resized to the sequence in-plane resolution voxel size $1 \times 1 \times 1$ using *resize_img* function with Matlab.

2.3.2. MRI preprocesing

MRI images were processed with Statistical Parametric Mapping (SPM) software (SPM8; Wellcome Trust Centre for Neuroimaging; University College London, UK). For MRI VBM analysis, we used the VBM8 package (http://dbm.neuro.uni-jena.de/vbm8/). T1-weighted brain anatomic images were segmented using a unified segmentation procedure (Ashburner and Friston, 2005). For tissue segmentation a gray and white matter study-specific template (total of 164 volumes) was generated using the Diffeomorphic Anatomical Registration Through Exponentiated Lie Algebra algorithm (Ashburner and Friston, 2005). This analysis concludes with the application of a spatial constraint to the segmented tissue probability maps, based on a Hidden Markov Random Field model (Cuadra et al., 2005). We set 0.1 and 0.2 thresholds for gray matter and white matter, respectively. Subsequently, each image was spatially normalized into the standard space of the Montreal Neurological Institute template (Template-1_IXI550_mini152.nii). Image normalization included both linear components and nonlinear transformations, which take into account individual regional differences in brain anatomy. A "Clean-up any partitions" procedure, particularly useful for atrophic brains, was implemented using conditional dilations and erosions to better differentiate gray matter and white matter. We used "Bias corrected image" for quality control and also to create an average image of all normalized T1 images. Because spatial normalization expands or contracts some brain regions, modulation to gray matter and white matter was applied, scaling by the amount of contraction, to preserve the total amount of gray matter and white matter of the original images. The resulting gray matter and white matter images were modulated to correct individual brain size. Finally, images were smoothed with a Gaussian kernel (FWHM of 8 mm for gray matter).

2.3.3. Neuroimaging cross-sectional analysis

For gray matter and white matter volumetric voxelwise analyses, we used statistical parametric mapping (SPM8) based on the General Linear Model. We used 4 different design matrices with a full factorial design. An ANOVA for the separate set analyses with the factor "subgroup" with age and gender as nuisance variables; another ANOVA was performed to determine whether there were volumetric differences owed to any of the 2 clinical status (MCI and AD) in the ADNI1 set; a third ANOVA for analyzing jointly the 2 sets with the factor "subgroup" with age and gender as nuisance variables; and a 2-way ANOVA for the analyses between sets with 2 factors "set" and "subgroup" with age and gender as nuisance variables. The latter matrix was used for the conjunction analysis.

2.3.3.1. Separated gray matter volumetric analysis of Spanish and ADNI1 sets. Initially, we assessed gray matter volumetric differences between AD/MCI p.R47H carriers, AD/MCI p.R47H noncarriers, and cognitively intact p.R47H noncarriers of the Spanish set. For this purpose, we conducted a full factorial analysis, an ANOVA with a factor "subgroup" with 3 levels (AD/MCI p.R47H carriers, AD/MCI p.R47H noncarriers, and cognitively intact p.R47H noncarriers). After determining a significant main effect of factor "subgroup", pairwise analyses were carried out by means of Statistical Parametric Mapping t test (SPM-t) comparisons. The statistical threshold used was $p < 0.05$ familywise error (FWE) cluster wise corrected ($p = 0.001$ cluster-defining threshold, $t = 3.17$).

In a second step, we performed the same full factorial analysis for the ADNI1 set as followed for that of the Spanish sample. The contrasts analyzed were the following: AD/MCI p.R47H carriers versus cognitively intact AD/MCI p.R47H noncarriers, AD/MCI p.R47H noncarriers versus cognitively intact AD/MCI p.R47H noncarriers, and AD/MCI p.R47H carriers versus AD/MCI p.R47H noncarriers. The same statistical threshold was used for SPM-t comparisons $p < 0.05$ FWE cluster wise corrected (cluster-defining threshold, $p = 0.001$, corresponding to $t = 3.24$ for the ADNI1 set).

2.3.3.1.1. Analysis of the presence of volumetric differences between AD and MCI subjects in ADNI1 set. To determine whether the clinical status of subjects (MCI and AD) could influence the results of ADNI1 set VBM analysis, we conducted a full factorial analysis for the ADNI1 set with factors: "group" with 2 levels (AD/MCI p.R47H carriers and AD/MCI p.R47H noncarriers), "clinical status" with 2 levels (AD and MCI), and their interaction "group $\times$ clinical status."

2.3.3.2. Analysis of intra-sample set specific morphometric differences between subgroups. To analyze jointly both sets, we performed a new factorial analysis to determine homogeneity among subgroups: 2-way ANOVA with a factor "set" of 2 levels (Spanish and ADNI1 sets) and a factor "group" with 3 levels (AD/MCI p.R47H carriers, AD/MCI p.R47H noncarriers, and cognitively intact p.R47H noncarriers). Age at the time of the brain MRI scan and gender were considered as nuisance variables. To evaluate the presence of gray matter loss differences between the homologous subgroups from each set, the following SPM-t pairwise analyses were carried out: AD/MCI p.R47H carriers from Spanish set versus AD/MCI p.R47H carriers from ADNI1 set and AD/MCI p.R47H noncarriers from Spanish set versus AD/MCI p.R47H noncarriers from ADNI1 set. This analysis showed no intra-sample set specific morphometric differences.

2.3.3.3. Conjunction analysis of Spanish and ADNI1 sets. We also performed a conjunction analysis with each subgroup of both sets to display statistically and topographically the maps of the common gray matter loss in both sets. For that, 3 new contrasts per data set were generated: AD/MCI p.R47H carriers versus AD/MCI p.R47H noncarriers, AD/MCI p.R47H carriers versus cognitively intact p.R47H noncarriers, and AD/MCI p.R47H noncarriers versus cognitively intact p.R47H noncarriers. Each pair of t contrasts (1 for each data set) was included in a separate conjunction analysis, following the method described by Friston (Friston et al., 2005). Statistical significance was corrected for $p < 0.05$ FWE cluster wise corrected (cluster-defining threshold, $p = 0.001$ and $t = 1.87$).

2.3.3.4. Joint analysis. Finally, a joint analysis of the 2 data sets was performed considering their homologous subgroups (AD/MCI p.R47H carriers, AD/MCI p.R47H noncarriers, or cognitively intact p.R47H noncarriers) to obtain a higher statistical power. We performed a full factorial analysis: an ANOVA with the factor "subgroup" of 3 levels (AD/MCI p.R47H carriers, AD/MCI p.R47H noncarriers, and cognitively intact p.R47H noncarriers). Ages at the time of the brain MRI scan and gender were considered as nuisance variables. The factor "subgroup" was significant. The following post hoc pairwise SPM-t comparisons were carried out: AD/MCI p.R47H carriers versus cognitively intact p.R47H noncarriers, AD/MCI p.R47H noncarriers versus cognitively intact p.R47H noncarriers, and AD/MCI p.R47H carriers versus AD/MCI p.R47H noncarriers. Statistical significance was assessed with an FWE cluster wise corrected p threshold < 0.05 (cluster-defining threshold, $p = 0.001$ and $t = 3.14$).

Leukoaraiosis, defined as the presence of hyperintense white matter lesions in both T2-weighted and fluid attenuated inversion recovery MRI sequences, was measured using the Scheltens semiquantitative visual rating scale (Scheltens et al., 1993). Because basal ganglia calcifications were previously described in Nasu-Hakola patients (Klunemann et al., 2005), the presence of brain

calcifications was screened visually. We performed the same full factorial analysis to assess white matter volumetric changes as described for gray matter contrasts.

3. Results

3.1. Clinical and neuropsychological findings

3.1.1. Spanish set

AD p.R47H carriers developed forgetfulness (7 of 9) and depression (2 of 9) as the main starting symptoms. During the first 2 years of the disease onset, minor depression and other psychiatric symptoms such as personality changes, anxiety, paranoia, or fears appeared more frequently in AD p.R47H carriers compared with AD noncarriers ($p < 0.05$). Early spatial disorientation (8 of 9) and apraxia (9 of 9) were also reported often. Indeed, significant statistical differences were observed in the number of p.R47H carriers presenting with apraxia compared with noncarriers ($p < 0.05$; Table 2). Parkinsonian signs were more frequent in AD p.R47H carriers (66.7%) than AD p.R47H noncarriers (14.6%, $p < 0.05$). Other neurologic symptoms less frequently observed among AD p.R47H carriers were somatic complaints (5 of 9), sleep apnea (3 of 9), myoclonus (2 of 9), seizures (1 of 9), insomnia (1 of 9), restless legs syndrome (1 of 9), and somniloquism (1 of 9). Clinical symptoms could not be evaluated in ADNI cohort because these data were not specifically recorded in ADNI1 subjects.

3.1.2. Both sets

Among 93 AD and/or MCI patients, MMSE scores were significantly lower in the p.R47H carriers group than in AD p.R47H noncarriers (mean 18 vs. 21.6, $p < 0.05$; Table 1). However, the conditional logistic model showed no statistically significant association of any of the neuropsychological tests with the *TREM2* p.R47H status.

3.2. MRI findings

SWI-MRI sequences showed no brain calcifications or cerebral hemosiderin deposits in any p.R47H carrier. The degree of leukoaraiosis measured by the Scheltens scale showed similar scores between AD/MCI p.R47H carriers (mean = 7.69, range: 0–21) and AD/MCI noncarriers (mean = 9, range: 0–37; Table 1).

3.2.1. Independent VBM analyses

3.2.1.1. Spanish set. The results of the ANOVA with a factor "subgroup" with 3 levels (AD/MCI p.R47H carriers, AD/MCI p.R47H noncarriers, and cognitively intact p.R47H noncarriers) showed a significant main effect ($F = 7.44$). Pairwise SPM-t between AD *TREM2* p.R47H carriers versus cognitively intact p.R47H noncarriers showed gray matter loss among AD *TREM2* p.R47H carriers in bilateral middle orbitofrontal regions and left parietal lobe (angular and supramarginal gyri) and right hippocampus. Additionally, a lower volume in subcortical regions such as bilateral thalamus and putamen was observed among AD *TREM2* p.R47H carriers. Gray matter loss was also located in the left middle temporal gyrus, inferior parietal regions, and bilaterally, in the thalamic regions. For AD *TREM2* p.R47H carriers versus AD *TREM2* p.R47H noncarrier contrast, we found a lower gray matter volume in right orbitofrontal regions (Fig. 1S and Supplementary Table 1). White matter VBM showed no significant differences in any of the 3 contrasts described previously.

3.2.1.2. ADNI1 set. To replicate the findings of the VBM analysis of the Spanish sample, the ADNI1 set was also analyzed separately with an ANOVA following a similar design to the Spanish set. There was a significant main effect of factor "subgroup" ($F = 7.88$). Pairwise analyses *t* test (SPM-t) of ADNI1 AD/MCI *TREM2* p.R47H carriers versus cognitively intact p.R47H noncarriers contrast not only showed a lower gray matter volume in rectal gyrus and temporal regions but also in the subcortical regions including the right caudate nucleus, putamen, pallidum, amygdala, and hippocampus. Other clusters with substantial gray matter loss were located bilaterally in the middle and superior temporal gyri. The largest gray matter loss was observed in the right temporal pole. In addition, there was a significant gray matter volume decrease in the middle frontal and cingulate gyri, superior and inferior parietal cortex and precuneus. At subcortical level, putamen and cerebellar vermis were the most affected regions. Finally, in the AD/MCI *TREM2* p.R47H carriers versus AD/MCI *TREM2* p.R47H noncarriers contrast, a nonsignificant gray matter loss in bilateral orbitofrontal regions was observed (Fig. 1S and Supplementary Table 2). For white matter volumetric analysis, as observed in the Spanish set analysis, we found no statistically significant differences between subgroups across the ADNI1 set.

3.2.1.2.1. Analysis of the presence of volumetric differences between AD and MCI subjects in ADNI1 set. Because we found no differences in the comparison of AD/MCI TREM2 p.R47H carriers versus AD/MCI TREM2 p.R47H noncarriers of the ADNI1 set, we conducted an additional analysis to assess the influence of diagnostic groups (MCI and AD) on the results. None of the factors (group, clinical status, or the interaction) were significant ($F = 13.89$, data not shown) suggesting that cerebral gray matter loss was similar in MCI and AD subjects. Thus, we concluded that the inclusion of MCI subjects along with AD subjects in the analysis would not change the results of the ADNI1 contrast.

3.2.2. Analysis of intra-sample set specific morphometric differences between subgroups

3.2.2.1. Factorial analysis between Spanish and ADNI1 sets. Regarding the factorial analysis using a 2-way ANOVA to determine the homogeneity of the data sets, the main effect of the factor "set" revealed no statistical significance ($F = 7.24$), but the subgroup factor, as expected, was statistically significant ($F = 11.60$). Interaction of the factor "set" and/or factor "subgroup" was not statistically significant. Pairwise *t* test contrasts comparing homologous subgroups between sets: AD *TREM2* p.R47H carriers ADNI1 set versus AD *TREM2* p.R47H carriers Spanish set and AD *TREM2* p.R47H noncarriers ADNI1 set versus AD *TREM2* p.R47H noncarriers Spanish set were not significant. These results suggested that there were low chances of finding differences resulting from comparisons between AD/MCI *TREM2* p.R47H carriers, AD/MCI *TREM2* p.R47H noncarriers, and cognitively intact p.R47H noncarriers because of a set effect (Spanish vs. ADNI1).

3.2.2.2. Conjunction analysis of Spanish and ADNI1 sets. A conjunction analysis of Spanish and ADNI1 sets was performed using the aforementioned factorial analysis. We observed significant common areas of gray matter loss among the homologous pairs of subgroups of each set. When compared with cognitively intact p.R47H noncarriers, the AD/MCI p.R47H carriers (Spanish vs. ADNI1 sets) showed common gray matter loss in superior and inferior frontal regions, mesial temporal areas including amygdala, hippocampus, and superior and inferior parietal areas. Regarding subcortical structures, we found common decrease of the gray matter in thalamus, cerebellum and basal ganglia, specifically in putamen and pallidum (Supplementary material Table 3, Fig. 2A).

AD/MCI p.R47H noncarriers versus cognitively intact p.R47H noncarriers (Spanish vs. ADNI1 sets) showed common gray matter loss in hippocampus and amygdala together with frontal and parietal areas. At subcortical level common loss of gray matter volume was located in thalamus and cerebellum. (Supplementary material Table 3, Fig. 2BS).

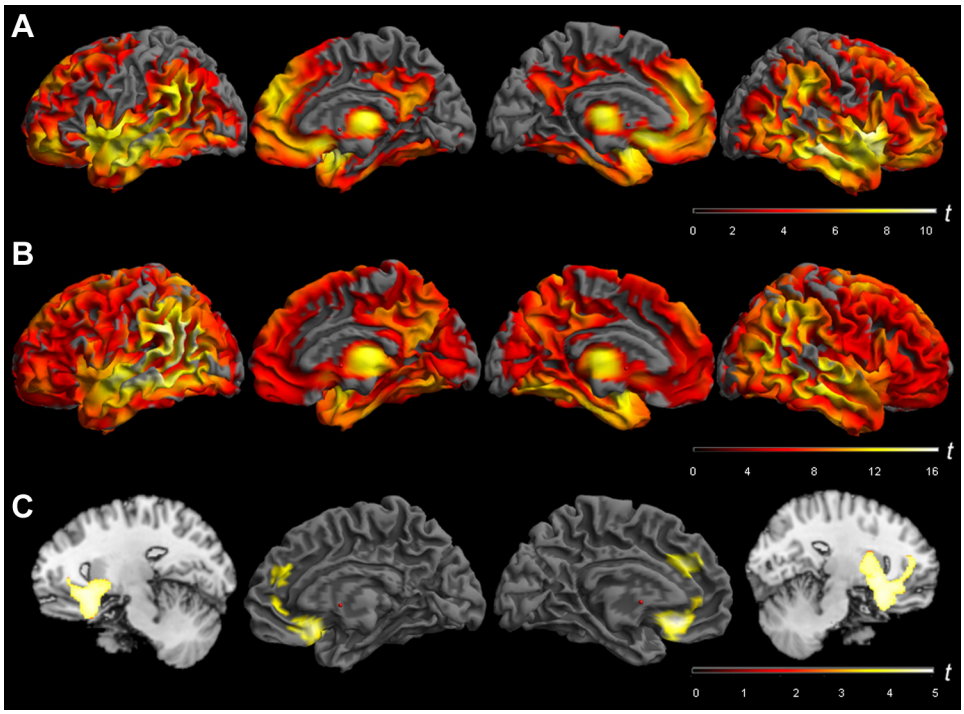

Fig. 1. Joint analysis displaying gray matter loss on the rendered surface of the brain, in the following contrasts: (A) Contrast AD/MCI *TREM2* p.R47H carriers versus cognitively intact *TREM2* p.R47H noncarriers. (B) Contrast AD/MCI no *TREM2* mutation carriers versus cognitively intact *TREM2* p.R47H noncarriers. (C) Contrast AD/MCI *TREM2* p.R47H carriers versus AD/MCI *TREM2* p.R47H noncarriers. The sagittal images had been added to display the basal ganglia gray matter loss. T-test scores scale. Threshold $p < 0.05$, FWE cluster wise $p < 0.001$. Abbreviations: AD, Alzheimer's disease; FWE, familywise error; MCI, mild cognitive impairment.

Finally, the common gray matter loss in both sets (Spanish and ADNI1) resulting from the contrast of AD *TREM2* R47H carriers versus AD *TREM2* R47H noncarriers was located in the orbitofrontal gyrus and anterior cingulate gyrus (Supplementary material Table 3, Fig. 2C).

3.2.3. Joint analysis

3.2.3.1. Gray matter VBM analysis. The ANOVA of the 2 sets joined showed a significant main effect of "subgroup" ($F = 7.22$).

3.2.3.1.1. Comparison between AD/MCI TREM2 p.R47H carriers versus cognitively intact p.R47H noncarriers. The 16 AD/MCI p.R47H carriers compared with 74 cognitively intact p.R47H noncarriers showed severe gray matter volume loss ($p < 0.05$ FWE cluster wise corrected) in the following regions: bilateral rectal gyri (orbitofrontal cortex), bilateral middle temporal, and amygdala. The maximum gray matter volume loss was observed in right rectal gyrus (t values of 10.28). Interestingly, parietal lobes were relatively spared in AD/MCI p.R47H carriers. With regard to the basal ganglia, gray matter loss was observed in both putamen and caudate nuclei among p.R47H carriers. The thalamic atrophic clusters showing greater degree atrophy were located in the ventral lateral nucleus, a relay nucleus with connectivity to the sensorimotor cortex (Fig. 1A and Supplementary Table 4).

3.2.3.1.2. Comparison between AD/MCI TREM2 noncarriers versus cognitively intact p.R47H noncarriers. We observed widespread gray matter loss in the 74 AD/MCI *TREM2* noncarriers compared with 74 cognitively intact p.R47H noncarriers ($p < 0.05$ FWE cluster wise corrected) with a predominant distribution in temporal and parietal lobes compared with frontal lobes. The temporal atrophic areas were located bilaterally in the middle temporal gyrus, where the maximum gray matter loss was found (t value = 15.56), as well as in mesial temporal areas including the hippocampus and amygdala. The hippocampal gray matter loss was more pronounced in the left side. This pattern was consistent with the results of previous VBM studies performed in AD-control series (Ishii et al., 2005). The second maximum region with gray matter loss outside the temporal lobes was located in the angular gyrus extending to the supramarginal gyrus predominantly on the left (t values of 15.14 and 14.94, respectively). Regarding subcortical structures, we found atrophy in the ventral lateral thalamic nuclei (Fig. 1B and Supplementary material Table 5).

3.2.3.1.3. Comparison between AD/MCI TREM2 p.R47H carriers versus AD/MCI TREM2 p.R47H noncarriers. We performed a direct comparison between 16 AD/MCI p.R47H carriers and 74 cognitively intact p.R47H noncarriers. In this comparison, we identified significant gray matter loss in bilateral anterior cingulate cortex, left

Table 4
Joint analysis. Volumetric gray matter loss contrast between AD/MCI *TREM2* p.R47H carriers versus AD/MCI *TREM2* noncarriers

Area	Side	BA	K	T	X	Y	Z
Frontal							
Rectal gyrus orbitofrontal cortex	R	11	7089	4.50	20	18	−14
	L			4.49	−9	26	−12
	R			4.28	12	29	−15
Superior frontal gyrus	L	6		4.09	−6	38	28
Anterior cingulate cortex	R	32		3.81	14	42	22
	R			3.42	15	48	10
	L			3.25	−6	41	1
Basal ganglia							
Putamen	R		7089	3.74	32	9	−5
	L			3.43	−10	7	−3
Caudate	R			3.28	13	9	−5
	L			3.43	−10	9	−3
Accumbens	R			3.15	12	8	−8
	L			3.59	−10	8	−8

Statistically significant gray matter loss. Side refers to laterality; BA refers to Brodmann Areas; K is the number of voxels per cluster, $p < 0.05$ FWE cluster wise corrected $p = 0.001$; T-test score; X,Y,Z indicates MNI coordinates.
Key: FWE, familywise error; L, left; R, right.

superior medial gyrus, and bilateral rostro-ventral putamen, caudate heads, and accumbens nuclei (Table 4 and Fig. 1C). These results suggest that the presence of *TREM2* p.R47H could be associated with a gray matter loss pattern with impairment of prefrontal and frontobasal regions with relative preservation of parietal lobes.

3.2.3.2. White matter VBM analysis. The same contrasts were performed to compare using voxel-based morphometry white matter brain volumes although no statistically significant differences were found among the groups (data not shown).

4. Discussion

In this study, we investigate whether the novel *TREM2* p.R47H variant is associated with particular phenotypical (clinical and neuroimaging) features compared with cognitively impaired and healthy subjects who were p.R47H noncarriers, as described for other genetic markers (Cruchaga et al., 2009; Goni et al., 2013). One important consideration is that the sets analyzed in our study were different with regard to the recruitment methods. The Spanish set is a clinical cohort-based case-control sample, whereas the ADNI1 is a longitudinal cohort with 3 different cognitive statuses (AD, MCI, and healthy controls). Thus, differences in the recruitment and in the clinical data collection made it difficult to fully compare certain clinical and neuropsychological variables.

With regard to the clinical characteristics of the Spanish set, most of the AD p.R47H carriers presented an initial amnesic syndrome, as observed for AD p.R47H noncarriers. However, AD p.R47H carriers showed depression and personality changes at early stages evolving rapidly into multidomain dementia. Visuospatial disorientation and parkinsonism appeared early in most of the AD p.R47H carriers. Indeed, the p.R47H variant has been also associated with Parkinson's disease (Benitez and Cruchaga, 2013; Rayaprolu et al., 2013), although these findings need further replication.

We found that the p.R47H carriers showed, especially in the Spanish sample, a multidomain severe cognitive progression associated with p.R47H and poor performance in MMSE (MMSE was $\leq$10 in 5 p.R47H AD carriers), suggesting that the p.R47H variant could lead in some cases to a more aggressive dementia. This impression is also supported by the increased temporal lobe atrophy found in a 24-month recent follow-up study among *TREM2* p.R47H mutation carriers (Rajagopalan et al., 2013). Although MMSE showed lower scores among AD/MCI *TREM2* p.R47H carriers compared with noncarriers (mean MMSE scores 18 and 21.6, respectively), the conditional logistic regression analysis showed no influence of p.R47H in any of the neuropsychological tests analyzed, suggesting that more studies are necessary to demonstrate that the TREM2 variants can lead to a more aggressive AD phenotype.

The *TREM2* p.R47H AD phenotype observed in the Spanish series has some similarities to the NHD phenotype (Guerreiro et al., 2013a, 2013b). Subjects with NHD usually appear to show a frontal-like syndrome, but asymptomatic NHD p.Q33X *TREM2* heterozygous carriers can display subclinical impairment of short and long term visuospatial memory as observed in our AD p.R47H series (Montalbetti et al., 2005). These results suggest that medial structures can be early impaired by loss-of-function *TREM2* heterozygous variants. On the other hand, few healthy p.R47H carriers have also been reported, indicating that p.R47H can behave as an AD risk variant with a large effect size but with incomplete penetrance (Jonsson et al., 2013). Indeed, only 10 of 18 p.R47H carriers had first-degree relatives with dementia. However, family segregation analysis and with longer follow-up studies of *TREM2* p.R47H carriers will help in clarifying this point.

VBM analyses were performed separately in the 2 sample sets. The analysis of the Spanish set showed a statistically significant gray matter loss in the AD TREM2 p.R47H carriers compared with cognitively intact p.R47H noncarriers in bilateral middle orbitofrontal regions and left parietal lobe (angular and supramarginal gyri), right hippocampus, and in subcortical regions such as thalamus and putamen (Fig. 1S and Supplementary Table 1). In AD, TREM2 p.R47H carriers versus AD TREM2 p.R47H noncarriers contrast, we found a lower gray matter volume in right orbitofrontal regions (Fig. 1S and Supplementary Table 1). To replicate the VBM analysis findings of the Spanish sample, we performed an independent analysis with the ADNI1 set. We found similar location of gray matter loss resulting from the comparison of AD/MCI *TREM2* p.R47H carriers versus cognitively intact p.R47H noncarriers in rectal gyrus, middle frontal, and cingulate gyri, superior and inferior parietal cortex and precuneus temporal regions, amygdala, hippocampus and in subcortical regions including the right caudate nucleus, putamen and pallidum. The AD *TREM2* p.R47H carriers versus AD *TREM2* p.R47H noncarriers contrast, showed gray matter loss in bilateral orbitofrontal regions but it did not survive the level of significance (Fig. 1S and Supplementary Table 2). The lack of replication of the results of the Spanish sample in the ADNI1 sample could be because of several reasons. The Spanish subjects were in more advanced AD stages (mean MMSE 12.7) and had a longer disease duration than the ADNI1 MCI/AD subjects (mean MMSE 23.3) because in the ADNI1 data set only subjects with mild AD were included. This observation suggests that *TREM2* p.R47H carriers could develop higher atrophy over time rates than noncarriers as supported by Rajagopalan et al. (2013) and thus increase differences in later disease stages. Another explanation for the lack of replication might be that the inclusion of MCI subjects could have diluted the results, but the lack of volumetric differences between MCI and AD subjects of ADNI1 suggested that most MCIs from ADNI1 were at preclinical AD stages.

To increase the sample, we confirmed the absence of intra-set statistical differences which allowed us to perform joint and conjunction analyses. Conjunction and joint analyses revealed substantial gray matter loss in orbitofrontal cortex and anterior cingulate cortex with relative preservation of parietal lobes in AD/MCI *TREM2* p.R47H carriers.

Thus, considering the analyses globally, the pattern of gray matter loss we observed in AD/MCI p.R47H carriers compared with healthy controls displayed some similarities and differences with regard to the typical gray matter loss pattern described for AD (Goni et al., 2013; Ishii et al., 2005). The largest atrophic clusters were located bilaterally in both hippocampal regions and the ventromedial prefrontal cortex followed by the anterior cingulate cortex, extending to the basal forebrain and putamen. The VBM direct comparison between of AD/MCI p.R47H carriers with AD/MCI *TREM2* p.R47H noncarriers showed significant bilateral gray matter loss in the ventromedial prefrontal cortex, including the orbitofrontal cortex, rostral anterior cingulate cortex, ventral striatum, and basal forebrain. The orbitofrontal clusters with gray matter loss correspond in the macaque brain to both the orbital network, involved in sensory integration and reward; and to the medial network, which modulates the visceral activity in response to affective stimuli (Hikosaka and Watanabe, 2000; Ongur and Price, 2000; Ongur et al., 2003). Interestingly, the most extensive connections of the orbitofrontal cortex are set with the mesial temporal lobe, including hippocampal field CA1, entorhinal and perirhinal cortices, and amygdala, indicating critical role of orbitofrontal cortex in integrative memory that links purpose and personal experience with contextual cues to produce judicious behavior (Cavada et al., 2000). In humans, the orbitofrontal cortex shows a richer functional parcellation with subdivisions connected to association

cortical areas such as prefrontal cortex and medial frontal limbic areas including anterior cingulate cortex and striatum (Kahnt et al., 2012). The impairment of regions involved in emotional control and the integration of multimodal sensory information as well as the impairment of the anterior cingulate cortex regions (Bush et al., 2000) could explain the early presentation of psychiatric symptoms, personality changes, and visuospatial disorientation observed in AD/MCI p.R47H carriers (Table 4; Fig. 1C). Interestingly, the frontal gray matter loss pattern observed in *TREM2* p.R47H carriers could explain the possible association of certain *TREM2* rare variants with clinical FTD (Lattante et al., 2013; Rayaprolu et al., 2013; Ruiz et al., 2014).

Although the putaminal atrophy was present in both carriers and noncarriers (see conjunction analysis comparing AD/MCI p.R47H noncarriers with cognitively intact AD/MCI p.R47H noncarriers, Fig. 1), the differential volume loss in AD/MCI p.R47H carriers included accumbens and nucleus basalis of Meynert area in addition to the rostro-ventral putamen and caudate heads. The decreased putamen gray matter loss volume observed has been also described in some familial AD series (Cash et al., 2013; Ryan et al., 2013). The areas of the ventral striatum are connected with the orbitofrontal cortex and anterior cingulate and receive dopaminergic input from the midbrain. In addition, such areas have a key role in reward processing. We hypothesize that degeneration of these nuclei could be related to the parkinsonian signs seen among some Spanish AD p.R47H carriers. Unfortunately, the lack of detailed clinical information in the ADNI1 series did not allow us to confirm these findings.

Leukoaraiosis is a common feature of NHD caused by *TREM2* recessive mutations (Paloneva et al., 2002). However, there were neither significant differences between the 2 AD/MCI groups in Sheltens scale (Table 1) nor clusters with white matter volume loss among *TREM2* p.R47H carriers, suggesting that larger AD *TREM2* series are needed to further evaluate the white matter subcortical impairment caused by the p.R47H variant. However, although the density of microglia in the normal human brain is greater in white matter than in gray matter (Mittelbronn et al., 2001), it is possible that among the p.R47H carriers AD brain, the impaired microglia function to prevent amyloid accumulation and clear cellular debris, may produce changes in the microglia mainly at cortical level with relative preservation of white matter glia.

In summary, our results suggest that frontobasal cortical regions could be more susceptible to the deleterious biological effects of the *TREM2* p.R47H variant. We are aware that our results are preliminary, based on a limited sample size with no follow-up, which suggests that we have to interpret these results cautiously and wait for them to be confirmed in larger AD series.

Disclosure statement

The authors report no conflicts of interest.

Acknowledgements

The authors thank all participating subjects and their relatives for their contribution to the study. They thank Drs Francisco Guillen-Grima and Marta Vidorreta for their statistical assessment. This work was supported by grants to Pau Pastor from the Department of Health of the Government of Navarra, Spain Grant # for "Government of Navarra" is 40001144 (refs.13085 and 3/2008) and from the UTE project FIMA, Spain. Elkin O Luis is supported by an Education Department grant from Government of Navarra (2011–2014). Cristina Razquin holds a "Torres Quevedo" fellowship from the Spanish Ministry of Science and Technology, co-financed by the European Social Fund. Genotyping for the R47H variant in the Spanish and Alzheimer's Disease Neuroimaging Initiative (ADNI) samples was supported by National Institutes of Health grants (R01-AG044546 and P30-NS069329), the Alzheimer Association (NIRG-11–200110), and the American Federation for Aging Research (Carlos Cruchaga). Data collection and sharing for this project were funded by the Alzheimer's Disease Neuroimaging Initiative (ADNI) (National Institutes of Health Grant U01 Ag024904). ADNI is funded by the National Institute on Aging, the National Institute of Biomedical Imaging and Bioengineering, and through generous contributions from the following: Alzheimer's Association; Alzheimer Drug Discovery Foundation; BioClinica, Inc; Biogen Idec; Bristol-Myers Squibb Foundation; Eisai; Elan Pharmaceuticals, Inc; Eli Lilly and Company; F. Hoffmann-La Roche Ltd and its affiliated company Genentech; GE Healthcare; Innogenetics, N.V.; IXICO Ltd; Janssen Alzheimer Immunotherapy Research & Development, LLC.; Johnson & Johnson Pharmaceutical Research & Development LLC.; Medpace, Inc; Merck & Co, Inc; Meso Scale Diagnostics, LLC.; NeuroRx Research; Novartis Pharmaceuticals Corporation; Pfizer; Piramal Imaging; Servier; Synarc Inc; and Takeda Pharmaceuticals North America. The Canadian Institutes of Health Research is providing funds to support ADNI clinical sites in Canada. Private sector contributions are facilitated by the Foundation for the National Institutes of Health (www.fnih.org). The grantee organization is the Northern California Institute for Research and Education, and the study is coordinated by the Alzheimer's Disease Cooperative Study at the University of California, San Diego. ADNI data are disseminated by the Laboratory for Neuro Imaging at the University of California, Los Angeles. This research was also supported by National Institutes of Health grants P30 AG010129 and K01 AG030514.

Appendix A. Supplementary data

Supplementary data associated with this article can be found, in the online version, at http://dx.doi.org/10.1016/j.neurobiolaging.2014.06.007.

References

Ashburner, J., Friston, K.J., 2005. Unified segmentation. Neuroimage 26, 839–851.
Benitez, B.A., Cruchaga, C., 2013. TREM2 and neurodegenerative disease. N. Engl. J. Med. 369, 1567–1568.
Benitez, B.A., Cooper, B., Pastor, P., Jin, S.C., Lorenzo, E., Cervantes, S., Cruchaga, C., 2013. TREM2 is associated with the risk of Alzheimer's disease in Spanish population. Neurobiol. Aging 34, 1711 e15-7.
Bouchon, A., Dietrich, J., Colonna, M., 2000. Cutting edge: inflammatory responses can be triggered by TREM-1, a novel receptor expressed on neutrophils and monocytes. J. Immunol. 164, 4991–4995.
Bush, G., Luu, P., Posner, M.I., 2000. Cognitive and emotional influences in anterior cingulate cortex. Trends Cogn. Sci. 4, 215–222.
Cady, J., Koval, E.D., Benitez, B.A., Zaidman, C., Jockel-Balsarotti, J., Allred, P., Baloh, R.H., Ravits, J., Simpson, E., Appel, S.H., Pestronk, A., Goate, A.M., Miller, T.M., Cruchaga, C., Harms, M.B., 2014. TREM2 variant p.R47H as a risk factor for sporadic amyotrophic lateral sclerosis. JAMA Neurol. 71, 449–453.
Cash, D.M., Ridgway, G.R., Liang, Y., Ryan, N.S., Kinnunen, K.M., Yeatman, T., Malone, I.B., Benzinger, T.L., Jack Jr., C.R., Thompson, P.M., Ghetti, B.F., Saykin, A.J., Masters, C.L., Ringman, J.M., Salloway, S.P., Schofield, P.R., Sperling, R.A., Cairns, N.J., Marcus, D.S., Xiong, C., Bateman, R.J., Morris, J.C., Rossor, M.N., Ourselin, S., Fox, N.C., Dominantly Inherited Alzheimer Network (DIAN), 2013. The pattern of atrophy in familial Alzheimer disease: volumetric MRI results from the DIAN study. Neurology 81, 1425–1433.
Cavada, C., Company, T., Tejedor, J., Cruz-Rizzolo, R.J., Reinoso-Suarez, F., 2000. The anatomical connections of the macaque monkey orbitofrontal cortex. A review. Cereb. Cortex 10, 220–242.
Crane, P.K., Carle, A., Gibbons, L.E., Insel, P., Mackin, R.S., Gross, A., Jones, R.N., Mukherjee, S., Curtis, S.M., Harvey, D., Weiner, M., Mungas, D., 2012. Development and assessment of a composite score for memory in the Alzheimer's Disease Neuroimaging Initiative (ADNI). Brain Imaging Behav. 6, 502–516.
Cruchaga, C., Fernandez-Seara, M.A., Seijo-Martinez, M., Samaranch, L., Lorenzo, E., Hinrichs, A., Irigoyen, J., Maestro, C., Prieto, E., Marti-Climent, J.M., Arbizu, J., Pastor, M.A., Pastor, P., 2009. Cortical atrophy and language network reorganization associated with a novel progranulin mutation. Cereb. Cortex 19, 1751–1760.

Cuadra, M.B., Cammoun, L., Butz, T., Cuisenaire, O., Thiran, J.P., 2005. Comparison and validation of tissue modelization and statistical classification methods in T1-weighted MR brain images. IEEE Trans. Med. Imaging 24, 1548–1565.

Folstein, M.F., Folstein, S.E., McHugh, P.R., 1975. "Mini-mental state". A practical method for grading the cognitive state of patients for the clinician. J. Psychiatr. Res. 12, 189–198.

Forabosco, P., Ramasamy, A., Trabzuni, D., Walker, R., Smith, C., Bras, J., Levine, A.P., Hardy, J., Pocock, J.M., Guerreiro, R., Weale, M.E., Ryten, M., 2013. Insights into TREM2 biology by network analysis of human brain gene expression data. Neurobiol. Aging 34, 2699–2714.

Friston, K.J., Penny, W.D., Glaser, D.E., 2005. Conjunction revisited. Neuroimage 25, 661–667.

Gibbons, L.E., Carle, A.C., Mackin, R.S., Harvey, D., Mukherjee, S., Insel, P., Curtis, S.M., Mungas, D., Crane, P.K., 2012. A composite score for executive functioning, validated in Alzheimer's Disease Neuroimaging Initiative (ADNI) participants with baseline mild cognitive impairment. Brain Imaging Behav. 6, 517–527.

Goni, J., Cervantes, S., Arrondo, G., Lamet, I., Pastor, P., Pastor, M.A., 2013. Selective brain gray matter atrophy associated with APOE epsilon4 and MAPT H1 in subjects with mild cognitive impairment. J. Alzheimers Dis. 33, 1009–1019.

Guerreiro, R., Wojtas, A., Bras, J., Carrasquillo, M., Rogaeva, E., Majounie, E., Cruchaga, C., Sassi, C., Kauwe, J.S., Younkin, S., Hazrati, L., Collinge, J., Pocock, J., Lashley, T., Williams, J., Lambert, J.C., Amouyel, P., Goate, A., Rademakers, R., Morgan, K., Powell, J., St George-Hyslop, P., Singleton, A., Hardy, J., 2013a. TREM2 variants in Alzheimer's disease. N. Engl. J. Med. 368, 117–127.

Guerreiro, R.J., Lohmann, E., Bras, J.M., Gibbs, J.R., Rohrer, J.D., Gurunlian, N., Dursun, B., Bilgic, B., Hanagasi, H., Gurvit, H., Emre, M., Singleton, A., Hardy, J., 2013b. Using exome sequencing to reveal mutations in TREM2 presenting as a frontotemporal dementia-like syndrome without bone involvement. JAMA Neurol. 70, 78–84.

Hakola, H.P., 1972. Neuropsychiatric and genetic aspects of a new hereditary disease characterized by progressive dementia and lipomembranous polycystic osteodysplasia. Acta Psychiatr. Scand. Suppl. 232, 1–173.

Hikosaka, K., Watanabe, M., 2000. Delay activity of orbital and lateral prefrontal neurons of the monkey varying with different rewards. Cereb. Cortex 10, 263–271.

Ishii, K., Sasaki, H., Kono, A.K., Miyamoto, N., Fukuda, T., Mori, E., 2005. Comparison of gray matter and metabolic reduction in mild Alzheimer's disease using FDG-PET and voxel-based morphometric MR studies. Eur. J. Nucl. Med. Mol. Imaging 32, 959–963.

Jin, S.C., Pastor, P., Cooper, B., Cervantes, S., Benitez, B.A., Razquin, C., Goate, A., Cruchaga, C., 2012. Pooled-DNA sequencing identifies novel causative variants in PSEN1, GRN and MAPT in a clinical early-onset and familial Alzheimer's disease Ibero-American cohort. Alzheimers Res. Ther. 4, 34.

Jonsson, T., Stefansson, H., Steinberg, S., Jonsdottir, I., Jonsson, P.V., Snaedal, J., Bjornsson, S., Huttenlocher, J., Levey, A.I., Lah, J.J., Rujescu, D., Hampel, H., Giegling, I., Andreassen, O.A., Engedal, K., Ulstein, I., Djurovic, S., Ibrahim-Verbaas, C., Hofman, A., Ikram, M.A., van Duijn, C.M., Thorsteinsdottir, U., Kong, A., Stefansson, K., 2013. Variant of TREM2 associated with the risk of Alzheimer's disease. N. Engl. J. Med. 368, 107–116.

Kahnt, T., Chang, L.J., Park, S.Q., Heinzle, J., Haynes, J.D., 2012. Connectivity-based parcellation of the human orbitofrontal cortex. J. Neurosci. 32, 6240–6250.

Klunemann, H.H., Ridha, B.H., Magy, L., Wherrett, J.R., Hemelsoet, D.M., Keen, R.W., De Bleecker, J.L., Rossor, M.N., Marienhagen, J., Klein, H.E., Peltonen, L., Paloneva, J., 2005. The genetic causes of basal ganglia calcification, dementia, and bone cysts: DAP12 and TREM2. Neurology 64, 1502–1507.

Lanier, L.L., Bakker, A.B., 2000. The ITAM-bearing transmembrane adaptor DAP12 in lymphoid and myeloid cell function. Immunol. Today 21, 611–614.

Lattante, S., Le Ber, I., Camuzat, A., Dayan, S., Godard, C., Van Bortel, I., De Septenville, A., Ciura, S., Brice, A., Kabashi, E., 2013. TREM2 mutations are rare in a French cohort of patients with frontotemporal dementia. Neurobiol. Aging 34, 2443, e1-2.

McKhann, G., Drachman, D., Folstein, M., Katzman, R., Price, D., Stadlan, E.M., 1984. Clinical diagnosis of Alzheimer's disease: report of the NINCDS-ADRDA Work Group under the auspices of Department of Health and Human Services Task Force on Alzheimer's Disease. Neurology 34, 939–944.

Melchior, B., Garcia, A.E., Hsiung, B.K., Lo, K.M., Doose, J.M., Thrash, J.C., Stalder, A.K., Staufenbiel, M., Neumann, H., Carson, M.J., 2010. Dual induction of TREM2 and tolerance-related transcript, Tmem176b, in amyloid transgenic mice: implications for vaccine-based therapies for Alzheimer's disease. ASN Neuro. 2, e00037.

Mittelbronn, M., Dietz, K., Schluesener, H.J., Meyermann, R., 2001. Local distribution of microglia in the normal adult human central nervous system differs by up to one order of magnitude. Acta Neuropathol. 101, 249–255.

Mohs, R.C., Knopman, D., Petersen, R.C., Ferris, S.H., Ernesto, C., Grundman, M., Sano, M., Bieliauskas, L., Geldmacher, D., Clark, C., Thal, L.J., 1997. Development of cognitive instruments for use in clinical trials of antidementia drugs: additions to the Alzheimer's Disease Assessment Scale that broaden its scope. The Alzheimer's Disease Cooperative Study. Alzheimer Dis. Assoc. Disord. 11 (Suppl 2), S13–S21.

Montalbetti, L., Ratti, M.T., Greco, B., Aprile, C., Moglia, A., Soragna, D., 2005. Neuropsychological tests and functional nuclear neuroimaging provide evidence of subclinical impairment in Nasu-Hakola disease heterozygotes. Funct. Neurol. 20, 71–75.

Morris, J.C., 1993. The Clinical Dementia Rating (CDR): current version and scoring rules. Neurology 43, 2412–2414.

Ongur, D., Price, J.L., 2000. The organization of networks within the orbital and medial prefrontal cortex of rats, monkeys and humans. Cereb. Cortex 10, 206–219.

Ongur, D., Ferry, A.T., Price, J.L., 2003. Architectonic subdivision of the human orbital and medial prefrontal cortex. J. Comp. Neurol. 460, 425–449.

Paloneva, J., Manninen, T., Christman, G., Hovanes, K., Mandelin, J., Adolfsson, R., Bianchin, M., Bird, T., Miranda, R., Salmaggi, A., Tranebjaerg, L., Konttinen, Y., Peltonen, L., 2002. Mutations in two genes encoding different subunits of a receptor signaling complex result in an identical disease phenotype. Am. J. Hum. Genet. 71, 656–662.

Parkin, A.J., Java, R.I., 1999. Deterioration of frontal lobe function in normal aging: influences of fluid intelligence versus perceptual speed. Neuropsychology 13, 539–545.

Patterson, N., Price, A.L., Reich, D., 2006. Population structure and eigenanalysis. PLoS Genet. 2, e190.

Rajagopalan, P., Hibar, D.P., Thompson, P.M., 2013. TREM2 and neurodegenerative disease. N. Engl. J. Med. 369, 1565–1567.

Rayaprolu, S., Mullen, B., Baker, M., Lynch, T., Finger, E., Seeley, W.W., Hatanpaa, K.J., Lomen-Hoerth, C., Kertesz, A., Bigio, E.H., Lippa, C., Josephs, K.A., Knopman, D.S., White 3rd, C.L., Caselli, R., Mackenzie, I.R., Miller, B.L., Boczarska-Jedynak, M., Opala, G., Krygowska-Wajs, A., Barcikowska, M., Younkin, S.G., Petersen, R.C., Ertekin-Taner, N., Uitti, R.J., Meschia, J.F., Boylan, K.B., Boeve, B.F., Graff-Radford, N.R., Wszolek, Z.K., Dickson, D.W., Rademakers, R., Ross, O.A., 2013. TREM2 in neurodegeneration: evidence for association of the p.R47H variant with frontotemporal dementia and Parkinson's disease. Mol. Neurodegener. 8, 10–19.

Reitz, C., Mayeux, R., 2013. TREM2 and neurodegenerative disease. N. Engl. J. Med. 369, 1564–1565.

Ruiz, A., Dols-Icardo, O., Bullido, M.J., Pastor, P., Rodriguez-Rodriguez, E., Lopez de Munain, A., de Pancorbo, M.M., Perez-Tur, J., Alvarez, V., Antonell, A., Lopez-Arrieta, J., Hernandez, I., Tarraga, L., Boada, M., Lleo, A., Blesa, R., Frank-Garcia, A., Sastre, I., Razquin, C., Ortega-Cubero, S., Lorenzo, E., Sanchez-Juan, P., Combarros, O., Moreno, F., Gorostidi, A., Elcoroaristizabal, X., Baquero, M., Coto, E., Sanchez-Valle, R., Clarimon, J., 2014. Assessing the role of the TREM2 p.R47H variant as a risk factor for Alzheimer's disease and frontotemporal dementia. Neurobiol. Aging 35, 444, e1-4.

Ryan, N.S., Keihaninejad, S., Shakespeare, T.J., Lehmann, M., Crutch, S.J., Malone, I.B., Thornton, J.S., Mancini, L., Hyare, H., Yousry, T., Ridgway, G.R., Zhang, H., Modat, M., Alexander, D.C., Rossor, M.N., Ourselin, S., Fox, N.C., 2013. Magnetic resonance imaging evidence for presymptomatic change in thalamus and caudate in familial Alzheimer's disease. Brain 136 (Pt 5), 1399–1414.

Scheltens, P., Barkhof, F., Leys, D., Pruvo, J.P., Nauta, J.J., Vermersch, P., Steinling, M., Valk, J., 1993. A semiquantative rating scale for the assessment of signal hyperintensities on magnetic resonance imaging. J. Neurol. Sci. 114, 7–12.

Shaw, L.M., Vanderstichele, H., Knapik-Czajka, M., Clark, C.M., Aisen, P.S., Petersen, R.C., Blennow, K., Soares, H., Simon, A., Lewczuk, P., Dean, R., Siemers, E., Potter, W., Lee, V.M., Trojanowski, J.Q., 2009. Cerebrospinal fluid biomarker signature in Alzheimer's disease neuroimaging initiative subjects. Ann. Neurol. 65, 403–413.

Takahashi, K., Rochford, C.D., Neumann, H., 2005. Clearance of apoptotic neurons without inflammation by microglial triggering receptor expressed on myeloid cells-2. J. Exp. Med. 201, 647–657.

Thelen, M., Razquin, C., Hernández, I., Gorostidi, A., Sánchez-Valle, R., Ortega-Cubero, S., Wolfsgruber, S., Drichel, D., Fliessbach, K., Duenkel, T., Damian, M., Heilmann, S., Slotosch, A., Lennarz, M., Seijo-Martínez, M., Rene, R., Kornhuber, J., Peters, O., Luckhaus, C., Jahn, H., Hüll, M., Rüther, E., Wiltfang, J., Lorenzo, E., Gascon, J., Lleó, A., Lladó, A., Campdelacreu, J., Moreno, F., Ahmadzadehfar, H., Dementia Genetics Spanish Consortium (DEGESCO), Fortea, J., Indakoetxea, B., Heneka, M.T., Wetter, A., Pastor, M.A., Riverol, M., Becker, T., Frölich, L., Tárraga, L., Boada, M., Wagner, M., Jessen, F., Maier, W., Clarimón, J., de Munain, A.L., Ruiz, A., Pastor, P., Ramirez, A., 2014. Investigation of the role of rare TREM2 variants in frontotemporal dementia subtypes. http://dx.doi.org/10.1016/j.neurobiolaging.2014.06.018.

Tombaugh, T.N., 2004. Trail Making Test A and B: normative data stratified by age and education. Arch. Clin. Neuropsychol. 19, 203–214.

Williams, B.W., Mack, W., Henderson, V.W., 1989. Boston Naming Test in Alzheimer's disease. Neuropsychologia 27, 1073–1079.

Yesavage, J.A., Brink, T.L., Rose, T.L., Lum, O., Huang, V., Adey, M., Leirer, V.O., 1982. Development and validation of a geriatric depression screening scale: a preliminary report. J. Psychiatr. Res. 17, 37–49.